Single-Ion Magnets with Giant Magnetic Anisotropy and Zero-Field Splitting

Miroslav Georgiev* and Hassan Chamati*

ACCESS | 📊 Metrics & More | 📰 Article Recommendations

ABSTRACT: The design of mononuclear molecular nanomagnets exhibiting a huge energy barrier to the reversal of magnetization have seen a surge of interest during the last few decades due to their potential technological applications. More specifically, single-ion magnets are peculiarly attractive by virtue of their rich quantum behavior and distinct fine structure. These are viable candidates for implementation as single-molecule high-density information storage devices and other applications in future quantum technologies. The present review presents the comprehensive state of the art in the topic of single-ion magnets possessing an eminent magnetization-reversal barrier, very slow magnetic relaxation and high blocking temperature. We turn our attention to the achievements in the synthesis of $3d$ and $4f$ single-ion

magnets during the last two decades and discuss the observed magnetostructural properties underlying the anisotropy behavior and the ensuing remanence. Furthermore, we highlight the fundamental theoretical aspects to shed light on the complex behavior of these nanosized magnetic entities. In particular, we focus on key notions, such as zero-field splitting, anisotropy energy and quantum tunneling of the magnetization and their interdependence.
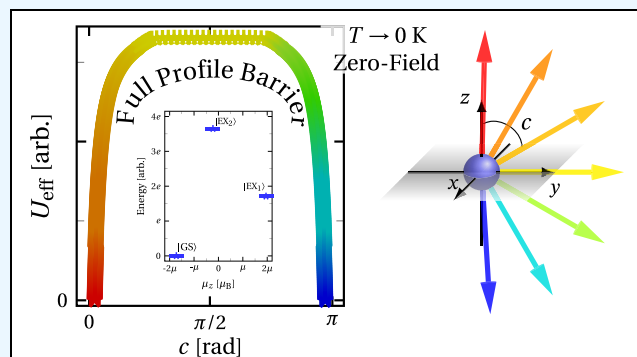
1. INTRODUCTION

For almost three decades the field of molecular magnetism has been a subject of great interest for experimentalists and theorists alike.[1] Since the synthesis of the first single-molecule magnet (SMM) was reported,[2] the number of synthesized SMMs has grown significantly. Exhibiting an energy barrier to the reversal of the magnetization of pure molecular origin, these building units of matter provide the ideal magnetic anisotropy (MA) property and manifesting molecular remanence that is useful for applications in quantum computing, molecule based information storage devices[3] and spintronics.[4] Of great potential for application are SMMs that exhibit a suppressed magnetization tunneling effect and possess a large or giant MA with high blocking temperature,[5] corresponding to the temperature below which the superparamagnetic behavior of a molecular nanomagnet vanishes. Hence, the system is in a blocked state with expected magnetic remanence, and a slow relaxation of the magnetization takes place. Notice that the blocking temperature is one of the main features under consideration with regard to future applications.

Especially intriguing with respect to their peculiar quantum magnetic behavior, distinct electronic spectra and fine structure (FS) are the mononuclear molecular nanomagnets, i.e. single-ion magnets (SIMs). Some of the most promising chemical elements for the synthesis of viable SIMs with considerable MA properties are the first-row transition metals[6] and lanthanides.[7]

Despite the fact that the $3d$ electrons interact strongly with the crystal field (CF) compared to the $4f$ ones, the design of SIMs based on either the first-row or lanthanide metals exclusively emphasizes two main features—a noninteger high-spin state and as low coordination number—as possible. Both features strongly promote the occurrence of large and even huge anisotropy energy and long-lasting relaxation of the magnetization. Any slow relaxation can then be directly controlled with the aid of an external magnetic field. Therefore, of great importance for the assembly of single-ion based devices is the production of stable, linear and high-spin Kramers complexes exhibiting a long magnetization-reversal time and as high as possible blocking temperature.[8]

While the race for the synthesis of stable and as low-coordinated as possible complexes nears its end,[9−11] the question regarding the manufacture of SIM devices continues to generate a great deal of interest within the scientific community. One of the most intriguing problems in

technological application is tightly related to adhesion effects. If successfully adsorbed on a surface,[12] SIMs with a well-pronounced magnetic hysteresis curve and, hence, strong remanence would be among the most reliable mononuclear based systems for technological implementation. The only competitors would be their smallest counterparts, or adatoms.[13] Note that the magnetic properties of adatoms can be described by the same theoretical methods used to analyze SIMs. In both cases, however, the processes of evaporation and diffusion along with the concomitant aggregation still pose a great challenge to be overcome.

In this mini-review we report the recent progress in the design of stable SIMs exhibiting large or giant MA and slow magnetic relaxation. We present some of the most prominent species among the 3d and 4f SIMs exhibiting extremely large energy barriers to the relaxation of the magnetization. The discussion primarily focuses on the theoretical aspects and future outlook. Note that all relevant quantities discussed hereafter are given by their effective values. In particular, we discuss the interrelationship between the zero-field splitting (ZFS) and MA, with a focus on the intricate correlation between anisotropy energy and energy level splitting pattern. A case of an ideal 3d^2 trigonal bipyramidal complex is considered in order to elucidate the genuine correspondence between both effects. Moreover, we briefly review a key case concerning the occurrence of huge ZFS in 3d^8 complexes and the possible emergence of unquenched orbital moment. The analysis is particularly focused on the recent studies of Ni^{2+} trigonal bipyramidal complexes.[14]

The rest of this mini-review is organized as follows. In Section 2 we review the progress achieved in the design and synthesis of 3d and 4f SIMs possessing giant magnetization-reversal barriers, slow zero-field magnetic relaxation and high-blocking temperature. Section 3 is devoted to a discussion on key theoretical aspects being of great significance for the future development of the research on SIMs. That includes a discussion on the interrelationship between ZFS, MA and quantum tunneling of the magnetization (QTM). Section 4 outlines the future development in the field of molecular magnetism.

2. IN THE PURSUIT OF THE LARGEST ENERGY BARRIER TO REVERSAL OF THE MAGNETIZATION

2.1. First-Row Transition Metal SIMs with Giant MA.
One of the first monometallic transition metal complexes found to exhibit field-induced slow magnetic relaxation with a magnetization-reversal barrier of approximately 42 cm^{-1} is the spin-two trigonal bipyramidal complex $[(\text{tpaMes})\text{Fe}]^-$ reported in 2010.[6d] Shortly thereafter, in the same year, studying the magnetic behavior of different Fe^{2+} based trigonal bipyramidal complexes, Harman et al.[6e] reported an even higher dc field dependent barrier. A prominent case is the compound $[\text{Na}(\text{solv})_n][(\text{tpa}^{\text{tert-butyl}})\text{Fe}]$, with anisotropy energy reaching 65 cm^{-1}. Such a value is among the highest observed for highly coordinated non-Kramers 3d ions. Nevertheless, for complexes with even total spin-magnetic quantum number m, the smaller m in the high-spin state, the lower the energy barrier to the relaxation of magnetization. In this respect, intriguing cases are the 3d^8 complexes with $m = 2$. Here, a barrier to the reversal of magnetization may not exist, since the mixing of CF basis states resulting from the spin–orbit coupling is either small or negligible, leading to the conservation of m as a good quantum number. Such a result is expected, since, for 3d^8 complexes, the subshell is almost completely filled and the probability to observe an unquenched orbital moment vanishes due to the

Pauli principle. One particular example is the case of a spin-one Ni^{2+} trigonal bipyramidal complex.[6f] Although there is a different ligand environment and distortion, the latter exhibits an almost two times smaller field induced magnetization-reversal barrier and similarly for the anisotropy energy compared to the Fe^{2+} based trigonal bipyramidal complexes.

Among the first transition metal complexes with extremely high anisotropy energies, however, are those composed of high-spin metal centers of odd spin quantum number and low coordination number. A particular example are the very rare cases of linearly coordinated Iron and Cobalt ions. A prominent species, introduced in 2013, is the homoleptic linear Fe$^+$ complex $[\text{Fe}(\text{C}(\text{SiMe}_3)_3)_2]^-$, with average Fe−C σ-bond distance of 2 Å, reported to have a large magnetization-reversal barrier.[9] The barrier is estimated to be approximately 226 cm^{-1}, which is extremely high for an iron based species. Moreover, in the absence of dc magnetic field the relaxation time is longer than 3 s for $T < 8$ K. When a dc field is applied, the relaxation time is prolonged to a few minutes. The corresponding hysteresis loop at 1.8 and 4.5 K along with the data showing the magnetization as a function of the temperature are depicted in Figure 1. The obtained blocking temperature, however, is T_B
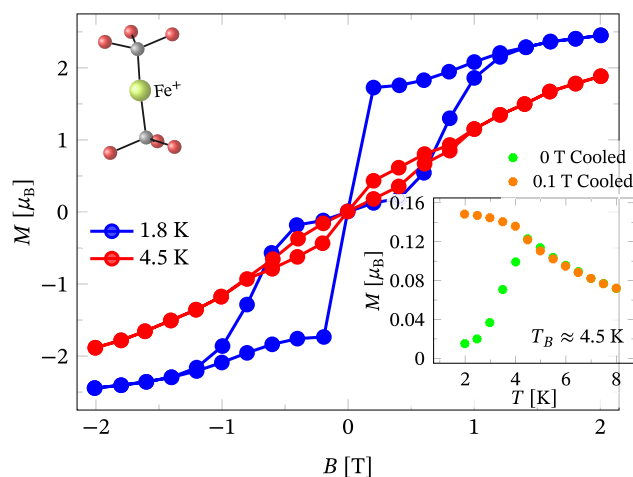
Figure 1. Magnetization as a function of the external magnetic field and temperature (inset) for the linear Fe$^+$ complex $[\text{Fe}(\text{C}(\text{SiMe}_3)_3)_2]^-$. The experimental data are provided in ref 9. The low-coordinated Iron shows a broad hysteresis loop obtained within an average sweep rate of 5 mT·s^{-1}. The blocking temperature is approximately 4.5 K, and the magnetization-reversal barrier is about 226 cm^{-1}. In addition, we depict a ball and stick representation of the local coordination, where the lime, gray and red colored spheres indicate the Iron, Carbon and Silicon atoms.

$\approx$ 4.5 K, which is far below that of conventional liquid nitrogen (77 K), making this single-ion magnet less suitable for application. Generally, in contrast to the highly coordinated Fe based SIMs, the slow relaxation of the magnetization in the two-coordinated species is observed in either the absence or presence of an external dc magnetic field. That makes them one of the most promising transition metal based SIMs for the design of linear complexes.

Other linear complexes showing a huge energy barrier to the relaxation of the magnetization and, hence, pronounced butterfly-like magnetic hysteresis were reported in 2017. These are the heteroleptic two-coordinated Co^{2+} based species reported in ref 11a. Although the π-bondings accommodate the

Table 1. Transition Metal and Lanthanide Based SIMs Possessing Extremely High Magnetization-Reversal Barrier E_{bar} Found in the Literature and Discussed in the Text along with Their Corresponding Blocking Temperature T_B and Relaxation Time τ at the Low-Temperature Range, T[a]

	Complexes	E_{bar} [cm^{-1}]	T_B [K]	τ [s]	T [K]	Ref.
	$[Fe(C(SiMe_3)_3)_2]^-$	226	4.5	$> 3^*$	< 8	9
	$[(sIPr)CoNDmp]$	413	7.5	$> 0.8^*$	< 12	11.a
	$[Dy(bbpen)Br]$	712	14	$> 10^*$	< 5	7.g
	$[Dy-5^*][B(C_6F_5)_4]$	1541	80	$> 10^4$	< 10	11.b
	$[Dy(Cp^{iPr4Me})_2][B(C_6F_5)_4]$	1468	62	$\gtrsim 10^3$	< 25	10
	$[Dy(O^tBu)_2(4\text{-phenylpyridine})_4]^+$	1442	8	$> 0.1^*$	< 5	7.e
	$RRRR$-Dy-$D_{6h}F_{12}$	1251	$\gtrsim 20$	$\geq 111^{**}$	≤ 5	11.c

[a]The local coordination of the listed SIMs is given in the first row. The asterisk symbol indicates that the results for τ, as reported in the corresponding references, are obtained in the absence of external dc magnetic field. The double asterisk symbol shows that the results are extracted from time decay magnetization measurements.

Nitrogen ligand very close to the metal center and the average Co−C distance is no larger than 1.96 Å, the overall CF effect remains weak. As a result, in the absence of external dc magnetic field the calculated relaxation of the magnetization barrier for all complexes is reported to lie in the range 297−413 cm^{-1}, or approximately 36−52 meV. The blocking temperature of the member with the highest relaxation barrier is a bit higher than expected. It is approximately two times the boiling temperature of liquid Helium (4.15 K). However, the corresponding relaxation time does not exceed more than 0.1 s at 12 K, with extrapolated saturation slightly less than 1 s. The results for these compounds are summarized in Table 1.

It is worthwhile to stress that the Co^{2+} complexes are 3d^7 systems. In other words, they have a highly occupied 3d subshell. As a result, even for an ideal CF symmetry, the zero-field magnetization-reversal barrier quickly vanishes as the coordination number increases. A completely different behavior to that of the aforementioned linear complexes are the recently investigated trigonal prismatic Co^{2+} compounds, introduced in the current year in ref 6g. Some of these complexes are reported to have field-induced slow magnetic relaxation with small zero-field anisotropy energy.

2.2. Lanthanide SIMs with Extremely High Magnetization-Reversal Barrier. Shortly after the first lanthanide SIMs were reported in 2003,[7f] researchers quickly realized the great potential of 4f elements in designing complexes that retain their magnetic states for a long period of time. Among all lanthanide SIMs the highest energy barrier to reversal of the magnetization and long relaxation time is held by Dy based complexes,[15] where the Dysprosium ion is in a high-spin state.

A fascinating case is the Br containing pentagonal bipyramidal Dy^{3+} complex with semilinear coordination introduced in 2016.[7g] The long Dy−Br ($\approx$ 2.85 Å) and Dy−N ($\approx$ 2.58 Å) distances from the equatorial plane promote the effect of spin−orbit coupling to the fine structure of the energy spectrum to a

large extent. That gives rise to a low-temperature, zero-field barrier's height of approximately 88.3 meV (712 cm^{-1}) and a broad 2 K magnetic hysteresis loop that closes at around T_B = 14 K for a powder sample. The resulting magnetization blocking duration is reported to be 41 s at 4 K. For the same temperature value and 0.2 T dc magnetic field, the time span prolongs up to 1825 s. As it may be expected, far lower is the magnetization-reversal barrier's value of the isostructural Cl species, with a Dy−Cl distance of approximately 2.68 Å. The barrier height is about 492 cm^{-1}, and the relaxation time in the absence of a dc field is reduced to a few milliseconds. These results are a classical example of how the stronger Cl ligand residing closer to the metal ion reduces the spin−orbit contribution to the observed MA properties and how the smaller atomic mass of Cl impacts the overall metal−ligand vibrational modes altering the magnetic relaxation.

The same magnetostructural dependencies are evident from the magnetic behavior of three hexagonal bipyramidal Dy^{3+} SIMs reported in 2019.[7h] One of the three compounds, the cation $[Dy^{III}(L^{N6})(Ph_3SiO^-)_2]^+$ with the longest average Dy−N equatorial distance, exhibits the highest magnetization-reversal barrier at zero applied dc field. It is approximately equal to 781 cm^{-1}. The relaxation time, however, is much shorter than 0.1 s for T < 10 K in zero dc field, and the corresponding magnetic hysteresis vanishes for T > T_B = 4 K, with measurements taken on a powder sample. Pushing the limits of the hexagonal bipyramidal Dy complexes with the same local ligand environment and symmetry, in the same year Li et al.[7i] reported an even higher zero-field barrier. In the fourth member of the introduced family of complexes, the six Nitrogen equatorial ligands reside farther from the Dy ion than in the remaining members. Furthermore, the two axial Dy−O bonds are the shortest found. Accordingly, this member has the largest anisotropy energy within the presented family. The corresponding barrier's value is approximately 930 cm^{-1}. Nevertheless, this complex has a short

relaxation time and, hence, small hysteresis loop that quickly shrinks while approaching the blocking temperature at about 6 K.

There are few Dysprosium based complexes with extremely high single-ion anisotropy (SIA), see Table 1. One such a compound, studied and reported in 2018,[11b] is the Dy based metallocene cation axially coordinated by a pentamethylcyclopentadienyl ligand and a penta-iso-propylcyclopentadienyl ligand over distances of 2.296 and 2.84 Å, respectively. This complex has a barrier to the magnetization reversal of approximately 1541 cm^{-1}, a blocking temperature slightly above the liquid nitrogen one and a relaxation time around 50 s at 80 K. Accordingly, it exhibits a very broad magnetic hysteresis loop that slowly closes while approaching 70 K. In addition, during the same year, several metallocenium salts with similar local coordination and, hence, magnetic behavior were reported.[10] The magnetization-reversal barriers' height ranges from 1280 to 1470 cm^{-1}, with blocking temperatures between 30 and 70 K. Accordingly, a slow magnetic relaxation is observed even for temperatures above 50 K, with a relaxation time span ranging from 10 to 100 s in a dc field. The magnetic hysteresis loops, along with susceptibility measurements, for the metallocenium species $[Dy(Cp^{iPr4Me})_2][B(C_6F_5)_4]$ are depicted in Figure 2.
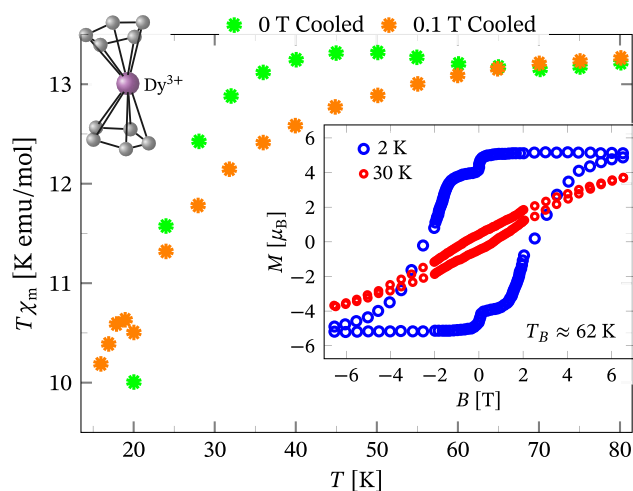
Figure 2. Molar susceptibility and magnetization data for the metallocenium salt $[Dy(Cp^{iPr4Me})_2][B(C_6F_5)_4]$ from ref 10. The isolated complexes $[Dy(Cp^{iPr4Me})_2]^+$ are found to exhibit one of the highest magnetization-reversal barriers ever reported among the known mononuclear nanomagnets. It is estimated to be approximately 1468 cm^{-1}. The inset depicts the corresponding magnetization hysteresis loop at two different temperatures, taken with the sweep rates of 3.1 mT s^{-1} and 13.2 mT s^{-1} at $B < 2$ T and $B > 2$ T, respectively. The complete data analysis from ref 10 shows that the loop closes at around 62 K. A ball and stick representation of the local coordination around the Dy atom (violet sphere) is also given. The gray colored spheres represent the Carbon atoms.

Recently, in 2021, two investigated types of highly coordinated Dy complexes have shown unusual features. Ding et al.[7e] reported a very large zero-field anisotropy energy in three octahedral complexes. For one of the members, the barrier's height reaches nearly 1442 cm^{-1}, which may be unexpected with regard to the local D_{4h} symmetry. Nevertheless, the zero-field measured relaxation time at 5 K is slightly above 0.1 s, and for a 20 mT s^{-1} sweep rate the observed magnetic hysteresis shows a

blocking temperature of approximately 8 K. Thus, although a large magnetization-reversal barrier is ensured by the very long Dy−N equatorial distances, with average value of approximately 2.5 Å, the presence of N ligands significantly suppresses the slow dynamics. On the other hand, in the same year the results introduced in ref 11c for two macrocyclic Dy^{3+} enantiomers pointed out that both complexes exhibit a low-temperature barrier of approximately 1251 cm^{-1} at zero dc field. It is also shown that these complexes demonstrate a very long relaxation time of almost 2500 s at 2 K and have a blocking temperature T_B > 20 K. Actually, this is one of the longest time periods for the reversal of the magnetization recorded at the few Kelvins regime for complexes with local D_{6h} symmetry. What makes these Kramers ion complexes so effective in retaining the magnetization state is the remote equatorial ligand environment and the weak contribution of the metal−ligand vibrational modes to the mixing of low-lying energy eigenstates. Both complexes have an average Dy−N distance of the hexagonal plane of approximately 2.68 Å. For more details on the bond lengths and angles, see the Supporting Information provided in ref 11c. The same magnetostructural correlations are further evident from the most recently studied macrocycle Dy^{3+} complexes reported quite recently in ref 11d. The study shows and confirms how the distant Dy−N equatorial CF affects the magnetization-reversal dynamics. The focus lies on two species distinguishable with respect to the Dy−N distances, reported to have energy barriers' heights of approximately 1204 and 1168 cm^{-1}. The most recent case of low-coordinated Dy^{3+} SIM reported in ref 11e, shown to possess a large energy barrier to the reversal of magnetization, is definitely another prominent example for the progress made in the design of mononuclear nanomagnets. The occurrence of two long Dy−N distances and one very long Dy−I distance gives rise to an energy barrier height of approximately 1237 cm^{-1} and a blocking temperature of about 20 K. All of the above-mentioned Dy based compounds stand as great examples for the advancement of chemical engineering of SIMs.

3. CRITICAL THEORETICAL ASPECTS

3.1. Models and Background. Despite witnessing tremendous progress in the synthesis, design and experimental characterization of SMMs[15,16] (see also refs 6a and 12a), their technological application is still beyond reach. Moreover, the detailed picture representing the magnetostructural correlations underlying MA and related dynamics is still not fully clear. Note that inconsistently complementing conceptually distinct theoretical methods to calculate the effect of different interactions strongly contribute to the overall ambiguity. Thus, any combination of different theoretical techniques to extract useful knowledge on the magnetostructural dependencies could end up as a nonconsistent theoretical approach that may yield nongenuine computational output.

Some of the most elusive representations that may mislead research, for example, arise from the phenomenological superposition of incompatible with respect to their physical background microscopic effective spin models, with the aim to generate a single multispin Hamiltonian or introduce a giant spin one.[17,18] One multispin Hamiltonian that inconsistently combines microscopic effective spin models reads

$$\hat{H} = \sum_{i,j} J_{ij}\hat{s}_i \cdot \hat{s}_j + \sum_i \hat{s}_i \cdot \mathbf{D}_{ii} \cdot \hat{s}_i + \sum_{i,j} \mathbf{d}_{ij} \cdot (\hat{s}_i \times \hat{s}_j)$$

(1)

where $i \neq j$ run over all effective spin centers in the molecular nanomagnet, J_{ij} are the corresponding exchange couplings,[19] $\mathbf{D}_{ii}$ are the one-site traceless symmetric tensors[20] and $\mathbf{d}_{ij}$ are the vectors associated with the Dzyaloshinskii Moriya interactions,[21] i.e. the antisymmetric exchange ones. At a given moment of time, each one of the three terms in eq 1 is inconsistent with the two others and, thus, should be used individually. For stationary states, some exceptions might be the cases when each term acts within a separate Hilbert space, i.e. refers to a particular group of electrons, or to the same electrons at a different point in time. The ambiguity occurring from the improper combination of different complete effective spin models, especially the bilinear exchange Hamiltonian[19] with the conventional ZFS one,[20,22] is beyond the scope of this review and will be discussed in a separate paper.[14]

On the other hand, the direct definition[5,17,23] of a relation between molecular nanomagnets' FS parameters and the classical magnetocrystalline anisotropy parameters from the phenomenological theory of MA in solids[24−26] strongly misshapes our understanding about the underlying quantum magnetization-reversal processes. If not properly applied, this definition yields an inconsistent theoretical approach for calculating MA and, hence, an unjustified relation between the phenomenological anisotropy constant "K" and FS parameters such as the axial D and rhombic E ones used to characterize ZFS in transition metal complexes. As a result, some molecular nanomagnets, expected to exhibit large anisotropy energy due to precalculated large splitting parameters, may in contrary show negligible or no sign of slow relaxation of magnetization. Then in these cases an actual absence of anisotropy energy due to QTM may be misinterpreted as a fast tunneling of magnetization through an existing full profile magnetization-reversal barrier. To gain additional knowledge on this matter, with discussion given in terms of the conventional ZFS parameter, the reader may further consult refs 21, 25, and 27. Along these lines, we may add a possible confusion of CF splitting as a huge ZFS (see refs 28) or associating the occurrence of large or huge ZFS only to the spin−orbit coupling.

An important step forward in molecular nanomagnets' comprehensive theoretical characterization is the use of well-established methods within their self-consistent framework: for example, the perturbation method[22,29] incorporating the residual electronic repulsion approach that ensures the conventional irreducible representation of orbital states and the complete active space variational one[30] (see also ref 29b) based on the direct diagonalization technique. The accurate use of these methods will reduce the number of possible computational errors to the minimum. To some extent, ab initio reformulations of both methods alone have the potential to provide a genuine knowledge on the contribution of all relevant interactions to the ground state magnetic properties as well as the electronic spectra and the underlying electron−electron and electron−nuclei correlations. Furthermore, DFT[31] and CF/LF[32] methods may be separately applied to elucidate the effects of bonding and coordination, respectively. The adequate use of the above-mentioned methods would significantly facilitate the efforts in reducing the gaps between them and, hence, in suppressing nonphysical features in the studies.

In particular, most important features for the design of SIMs, adatoms or low-dimensional systems of well isolated complexes with extremely high MA are the CF symmetry, spin−orbit interactions of relativistic origin and the spin exchange

interactions. Having at hand either a perturbation or direct diagonalization self-consistent method to unequivocally determine the influence and interplay of these interactions on the fine structure associated with the ground state (FSG) would be of great benefit. As mentioned above, it is expected to get rid of any puzzlement that has a long-standing impact on our knowledge of the genuine behavior of SIMs.

3.2. Anisotropy Energy in SIMs. One puzzle that may arise and be counterproductive to gaining insight into the properties of mononuclear molecular magnets is generated by the intricate correlation between MA/SIA and the zero-field FSG. That interrelationship may embed the notion that within a zero-field FSG an anisotropy energy always exists and its highest value is proportional to the overall ZFS. Furthermore, there is a corresponding slow relaxation of magnetization that is suppressed by QTM.

The notion that MA/SIA is inextricably related to the presence of ZFS may be traced back to the use of the semiclassical approach in studying the magnetization-reversal in SIMs, when as a matter of fact some SIMs have distinct quantum magnetic behaviors. In this case the internal energy per single complex may not be directionally dependent and, hence, even in the presence of apparent ZFS an anisotropic behavior may be absent. One particular group of SIMs that behave quantum mechanically even at low magnetic fields includes all complexes with the total magnetic quantum number m being a good quantum number; that is, the square of total spin α component commutes with the system's total Hamiltonian, where α is the quantization axis. Accordingly, these are all complexes that have low-lying energy eigenstates represented as a superposition of equal by absolute value and opposite by sign magnetic quantum numbers. A trivial example are SIMs having the ground state $|\psi_0\rangle = \frac{1}{\sqrt{2}}(|-s\rangle + |s\rangle)$, where s is the maximal value of the total spin quantum number. Such SIMs may exhibit FSG but cannot generate a zero dc field magnetization-reversal barrier and do not show MA properties. That is because the quantum basis states $|-s\rangle$ and $|s\rangle$ are equally favorable by energy and most importantly the spin-reversal pathways involving all or some excited energy eigenstates with $|m| < s$ are not required by the laws of quantum mechanics, as it would be the case if the system is approximated to a classical one. Therefore, by virtue of the quantum oscillations between the states $|-s\rangle$ and $|s\rangle$, the energy gaps separating the ground state from the excited ones do not mediate the zero-field ground state magnetization dynamics. This is a conventional case of QTM, since the spin-reversal at zero or low field and low temperature occurs without any exchange of energy and contribution from the intermediate spin states. Consequently, the direction cosines and respective angles[26,33] (see also ref 20a) have discrete values, and at low temperatures the average internal energy of the system represented as a function of the direction angles has a discrete domain, D: $\{-\pi, 0, \pi\}$ and range, R: $\{0, 0, 0\}$. Hence, an anisotropy energy does not exist, and neither step-like nor continuous magnetization-reversal processes defined within the domain $D' = (-\pi, \pi)$ take place.

Hereon, focusing on a more realistic case demonstrating the absence of MA and hence anisotropic energy in the presence of a zero-field FSG, we consider a spin-one transition metal SIM. For the cases of lanthanide SIMs, the reader may consult refs 7a and d and the references therein.

We consider a system composed of indistinguishable homoleptic ideal trigonal bipyramidal $3d^2$ complexes. Each

complex is characterized by metal−ligand bond distances of 2 Å and ligand charge numbers equal to unity. The metal center's charge number is constrained to $Z = 9$ and the covalence factor to unity. The calculations are performed with the aid of the method presented in ref 30c. The ground state of the investigated complex is $|1\rangle$ as labeled in Figure 3(a). Given in
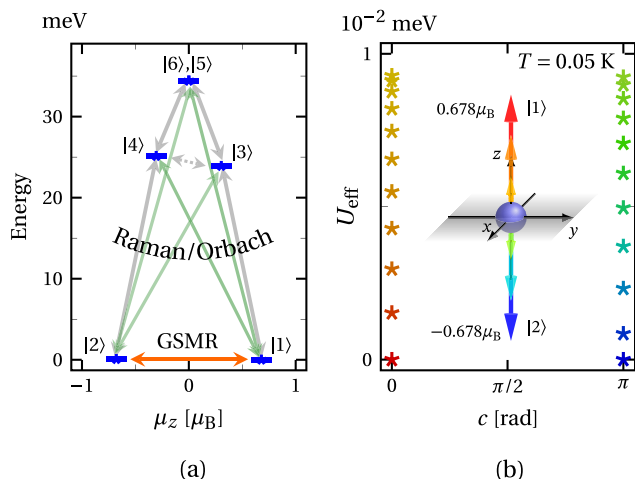
Figure 3. (a) Energy versus magnetic moment plot of the first six energy eigenstates, $|i\rangle$, $i = 1, ..., 6$, of an ideal trigonal bipyramidal $3d^2$ complex at zero field. The magnetic moment μ_z designates the expectation value of the total magnetic moment's z component. The z axis is parallel to the principal one. The values of all relevant parameters are given in Section 3.2. All arrows indicate possible pathways for the reversal of μ_z. The gray and green colored ones show those requiring an external energy source. The red one depicts the ground state magnetization-reversal GSMR dynamics. (b) Internal energy per single complex U_{eff} as a function of the direction angle c between the principle axis of the considered complex and the expectation value of its total magnetic moment. The corresponding vector is colored with the color map of the data for better visualization. As a function of the remaining two direction angles, U_{eff} is zero.

μ_B units, for the corresponding expectation values of the spin and orbital magnetic moments we have $\boldsymbol{\mu}_{1,s} = (0, 0, -1.34125)$ and $\boldsymbol{\mu}_{1,l} = (0, 0, 2.02009)$, respectively. Within the first exited state $|2\rangle$, of energy 7×10^{-2} meV, the respective expectation values are $\boldsymbol{\mu}_{2,s} = (0, 0, 1.34158)$ and $\boldsymbol{\mu}_{2,l} = (0, 0, -2.02054)$. Thus, we have an unquenched orbital moment occurring due to the ground state orbital degeneracy and lack of core orbitals, i.e. $E_{d_{xz}} - E_{d_{yz}} = 0$ and $E_{d_{x^2-y^2}} - E_{d_{xy}} = 0$. Moreover, we have huge energy gaps (see Figure 3(a)) partially resulting from the energy difference $E_{d_{xz}} - E_{d_{xy}} \approx 66$ meV.

Although the total ab initio ZFS is considerably large, approximately 282 cm^{-1} (≈ 35 meV), the zero-field magnetization-reversal barrier's height, calculated per single complex with respect to its principle axis, is no larger than 0.9×10^{-2} meV (shown in Figure 3(b)). Note that the barrier is not identically zero since $E_2 - E_1 \approx 7 \times 10^{-2}$ meV. Hence, neither the energy nor magnetization are directionally specific. In particular, the barrier's profile, i.e. the domain and range of the internal energy per single complex U_{eff}, shows that the magnetization-reversal is neither step-like nor continuous. In other words the magnetization per single ion decreases from 0.678 μ_B to zero and then further to -0.678 μ_B and vice versa without crossing the plane perpendicular to the principle axis. This is unlike the semiclassical and classical views of the magnetization dynamics,

where the total magnetic moment flips and the associated magnetization-reversal barrier has a well-defined "peak" that represents the maximal anisotropy energy value. In the considered case shown in Figure 3(b) the barrier's "peak" does not exist because the ground state dynamics of an individual complex's total magnetic moment depends only on the energy eigenstates $|1\rangle$ and $|2\rangle$ that are not a function of the $s = 0$ quantum basis states. The latter enter only into the superposition of the very high in energy excited energy eigenstates that are particularly related to the magnetization-reversal processes requiring an external energy source, such as the photon and phonon scattering and absorption/emission. Such dynamics is indicated by a red double arrow in Figure 3(a) and is referred to as QTM, since it does not require an intermediate state and applied external energy source. Thus, at $T = 0.05$ K, the associated first order phenomenological anisotropy constant per single complex is $K < 10^{-2}$ meV and the domains of the directional cosines are represented by the discrete set $\{-\pi, 0, \pi\}$. That is the case even at a few Kelvins.

Finally, the excited energy eigenstates $|3\rangle, ..., |6\rangle$ govern only direct or thermally activated magnetic excitations followed by Raman and/or Orbach relaxations[7j,5b] shown by double gray and green arrows in Figure 3(a). These processes may affect the magnetization state but do not define its ground state magnetic properties. Nevertheless, the Raman and Orbach relaxations may have a significant impact on the near ground state magnetization-reversal dynamics of complexes exhibiting a full profile barrier. The design of the latter is one of the main goals in the field of mononuclear nanomagnets, since QTM would be suppressed, giving rise to a step-like magnetization-reversal that can be properly manipulated by an external magnetic field. A model based on the diatomic molecule $[DyO]^+$ showing step-like magnetization-reversal through a thermally activated relaxation was introduced in ref 7d. The corresponding energy level diagram is depicted in Figure 4.

We would like to point out that for a large number of electrons, ligands and active space the probability to have a ground state represented as a superposition of all magnetic multiplets is larger. As a consequence, the corresponding
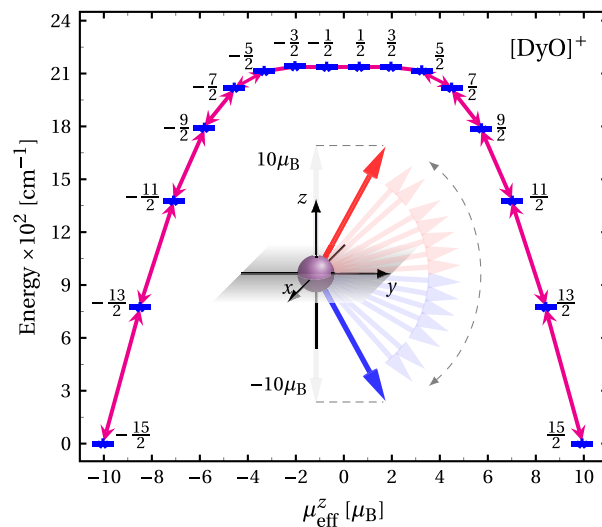
Figure 4. Energy versus magnetic moment plot of the idealistic diatomic system $[DyO]^+$, with a Dy−O bond distance of 1.74 Å. Data provided by ref 7d. The inset sketches the step-like reversal of the corresponding magnetic moment.

magnetization-reversal process may resemble a classical one. In this respect, the polynuclear molecular magnets stand as a notable instance for testing whether the corresponding principle holds.
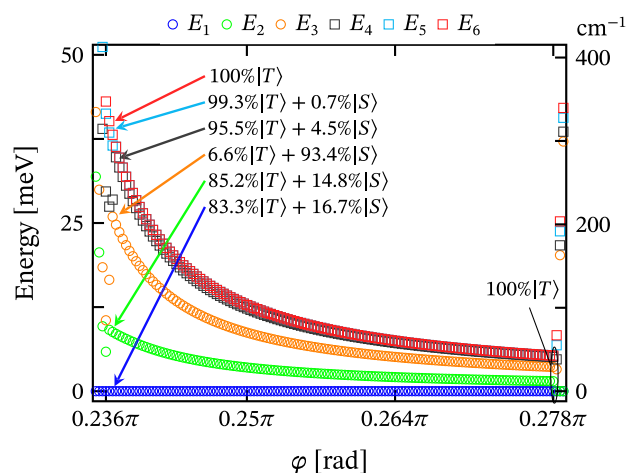
3.3. The Lack of Zero-Field FSG in Some SIMs. In the theory of transition metal complexes, there are cases when the absence of conventional ZFS is hindered by the emergence of nontrivial zero-field FS with an intricate interrelationship to MA. The most prominent cases that demonstrate how elusive the determination of true ZFS and its relation to MA can be are the complexes composed of metal ions with an almost completely filled valence subshell. Among the first-row transition metal SIMs, the Ni^{2+} trigonal bipyramidal complexes are a notable example.[34] A low-lying energy level sequence of a homoleptic slightly elongated trigonal bipyramidal complex, with Ni^{2+} metal center of charge number $Z = 12$, is shown in Figure 5(b). For

Studying the ground state magnetic properties of Ni^{2+} complexes, we consider the multiconfigurational approach discussed in ref 30b. We demonstrate that the only physical source that may lead to a huge ZFS in $3d^8$ complexes is the restricted mutual orbital motion of both unpaired electrons. The corresponding degrees of freedom are restricted by imposing a constraint over the phases φ related to the orbital states of the unpaired electrons. As a result of that constraint, the direct exchange interactions influence FSG by favoring the singlet configurations in addition to the triplet ones. The resultant superposition of singlet and triplet states lifts the excited energy levels from FSG to extreme values. FSG in the case of ideal trigonal bipyramidal geometry, with 2 Å bonds, Nickel's charge number $Z = 12$, ligands charge numbers and covalence factor equal to unity and values of the constraint, as a function of φ in the range $[0.2369\pi, 0.2789\pi]$, is depicted in Figure 6. The

Figure 5. First few low-lying energy levels of two Ni^{2+} complexes with slightly elongated axial bonds. (a) Octahedral coordination and (b) trigonal bipyramidal one. The values of all relevant parameters are provided in Section 3.3. All energy values are normalized such that the ground state one starts at zero.

Figure 6. Low-lying energy levels of an ideal trigonal bipyramidal Ni^{2+} complex as a function of the phase difference φ between the orbital states of both unpaired electrons. The values of all relevant model parameters are given in Section 3.3. The capital letters "S" and "T" stand for singlet and triplet, respectively. In contrast to the lack of FSG depicted in Figure 5 (b), here we observe a complex FSG resulting from the restricted mutual orbital motion of both unpaired electrons.

comparison the low-lying energy level sequence of the octahedral Ni^{2+} analog is depicted in Figure 5(a). The covalence factor $\kappa = 1$, and all ligands are considered to have a unity charge number. The axial and planar bond distances equal 2.1 and 2 Å, respectively. The energy spectra are calculated with the aid of an adapted to $3d^8$ systems exact diagonalization approach introduced in ref 30c. In both cases we have a highly spin degenerate ground state and excited spin multiplets being a component of FS far from the ground state due to the action of the CF. In other words, no zero-field FSG and unquenched orbital moment exist. Note that the occurrence of unquenched orbital moment in highly coordinated $3d^8$ complexes is not allowed by the Pauli principle. Therefore, a trigonal bipyramidal $3d^8$ complex, localized to a large extent around the metal center electrons, cannot exhibit huge ZFS and giant MA driven by the spin−orbit coupling alone. We would like to point out that the lack of ZFS is observed even for distorted trigonal bipyramidal structures, except the highly compressed and elongated bipyramidal cases for which the overall ZFS value does not exceed a few tens of cm⁻¹. Nevertheless, these complexes show no sign of spin−orbit driven anisotropy properties and, hence, no slow relaxation of the magnetization.

overall ZFS ranges from approximately 40 to 5.2 meV, or 322 cm⁻¹ to 42 cm⁻¹, respectively. The obtained ab initio energy level sequence near the boundary $\varphi \rightarrow 0.2369\pi$ could be effectively represented with the aid of the spin-sigma Hamiltonian[35] (see e.g. ref 30b for further details), given by

$$\hat{\mathcal{H}} = J(\hat{\boldsymbol{\sigma}}_1 \cdot \hat{\mathbf{s}}_2 + \hat{\boldsymbol{\sigma}}_2 \cdot \hat{\mathbf{s}}_1) \qquad (2)$$

where J is the corresponding effective intraexchange constant, for $i = 1, 2$, $\hat{\mathbf{s}}_i = (\hat{s}_i^\alpha)_{\alpha = \{x,y,z\}}$ is an effective spin-half operator and the sigma operator $\hat{\boldsymbol{\sigma}}_i = (\hat{\sigma}_i^\alpha)_{\alpha = \{x,y,z\}}$ is defined under the relation

$$\hat{\sigma}_i^\alpha |s, m\rangle_{n_s} = a_{s,n_s} \hat{s}_i^\alpha |s, m\rangle_{n_s}, \qquad n_s \in \mathbb{Z}_+$$

Here, a_{s,n_s} are real parameters and $|s, m\rangle_{n_s}$ are the eigenstates of eq 2, where $s = 0, 1$ and $m = 0, \pm 1$. Note that the conventional bilinear exchange model,[19] obtained within the approximation $a_{s,n_s} = 1, \forall s, n_s$, can account for only a fraction of that sequence. At the limit $\varphi \rightarrow 0.2789\pi$, FSG could be effectively represented by the effective ZFS Hamiltonians

$$\hat{H}_D = \hat{\mathbf{S}} \cdot \mathbf{D} \cdot \hat{\mathbf{S}}, \quad \hat{H}_{ZFS} = D\left(\hat{S}_z^2 - \frac{S(S+1)}{3}\right) + E(\hat{S}_x^2 - \hat{S}_y^2)$$

where $\hat{\mathbf{S}} = (\hat{S}_\alpha)$, $\alpha = x, y, z$ is the corresponding effective spin-one operator, $\mathbf{D}$ is a traceless symmetric tensor, with elements $D_{\alpha\beta} \in \mathbb{R}$, $\alpha, \beta = x, y, z$, and D and E are the axial and rhombic FSG parameters. Relations between the $\mathbf{D}$ tensor components and the conventional (D, E) ZFS parameters can be found in refs 20a, 22, and 32b.

The occurrence of FSG and particularly huge ZFS in Nickel based trigonal bipyramidal complexes is an ongoing discussion that has the potential to reshape part of the conventional understanding about the electron correlations governing the ground state magnetic properties of complexes composed of metals with a highly occupied $3d$ subshell. A thorough analysis of the ground state magnetic properties of $3d^8$ complexes will be published in a separate paper.[14] Therein we unravel the only possible physical terms upholding the probability of observing huge ZFS.

4. FUTURE OUTLOOK

Considering the constantly growing interest in engineering nanosized information storage devices operating on the boundary between quantum and classical physics, any experimental and theoretical progress in the field of molecular nanomagnetism would be of great significance. One of the main goals prior to the assembly of such devices would require the design of reliable SMMs, SIMs and low-dimensional units composed of adatoms or SIMs that possess the correct MA properties and, hence, remanence of pure molecular origin. In that respect, the last two decades have seen considerable progress that further fuels and ensures the future growth of the field. That includes the synthesis of many low-coordinated mononuclear molecular nanomagnets with exceptionally large magnetization-reversal barriers, blocking temperatures and relaxation time, fit for manipulation with an external magnetic field or a laser source. We review some of the most prominent cases based on $3d$ and $4f$ elements in Sections 2.1 and 2.2, respectively. Of course the realization of high-density magnetic storage devices based on SIMs or adatoms is tightly related to the processes of adsorption on a surface, which underline the other main goal that will power up future efforts in the field. Moreover, controlling the process of aggregation will pave the way of molecular nanomagnets' design to their technological implementation.

■ AUTHOR INFORMATION

Corresponding Authors

Miroslav Georgiev — *G Nadjakov Institute of Solid State Physics, Bulgarian Academy of Sciences, 1784 Sofia, Bulgaria;* orcid.org/0000-0003-0598-3360; Email: mgeorgiev@issp.bas.bg

Hassan Chamati — *G Nadjakov Institute of Solid State Physics, Bulgarian Academy of Sciences, 1784 Sofia, Bulgaria;* orcid.org/0000-0002-0831-6945; Email: chamati@issp.bas.bg

Complete contact information is available at:
https://pubs.acs.org/10.1021/acsomega.2c06119

Notes

The authors declare no competing financial interest.

Biographies

Miroslav Georgiev got his bachelor's degree in Physics from the "Paisii Hilendarski" University, Bulgaria, in 2012. In 2014 he graduated with a M.S. in Theoretical Physics from the same university. At the end of 2014 he joined the Theoretical Department at the Institute of Solid State Physics Bulgarian Academy of Sciences as a Ph.D. student and graduated in early 2019. His current research interests cover the field of molecular magnetism and low-dimensional spin systems with a focus on the theory studying all relevant phenomena.

Hassan Chamati got his Ph.D. and the research degree Doctor of Sciences in physics from the Institute of Solid State Physics, Bulgarian Academy of Sciences, where he has been acting as a Director since December 2015. He has been a Postdoctoral Fellow in many universities across Europe. He is a Full Professor and Head of the Theoretical Department at the same Institute. His main research interests are in the theory of Condensed Matter, including Soft Matter. He has published numerous papers in renowned international journals on quantum magnetism and computer modeling of materials and biomembranes. He established international collaborations with researchers from different countries. He served as Principal Investigator or team member in several research projects funded by national and international funding agencies.

■ ACKNOWLEDGMENTS

■ REFERENCES

(1) (a) Gatteschi, D.; Sessoli, R.; Villain, J. *Molecular Nanomagnets*; Oxford University Press: New York, 2006. (b) Winpenny, R. *Molecular Cluster Magnets*; World Scientific Series in Nanoscience and Nanotechnology; World Scientific, 2011; Vol. 3. (c) Gao, S., Ed. *Molecular Nanomagnets and Related Phenomena*; Structure and Bonding; Springer: Berlin, 2015; Vol. *164*. (d) Giansiracusa, M. J.; Gransbury, G. K.; Chilton, N. F.; Mills, D. P. Single-Molecule Magnets. In *Encyclopedia of Inorganic and Bioinorganic Chemistry*, 1st ed.; Scott, R. A., Ed.; Wiley, 2021; pp 1–21. (e) Wang, J.-H.; Li, Z.-Y.; Yamashita, M.; Bu, X.-H. Recent progress on cyano-bridged transition-metal-based single-molecule magnets and single-chain magnets. *Coord. Chem. Rev.* **2021**, *428*, 213617.

(2) (a) Caneschi, A.; Gatteschi, D.; Sessoli, R.; Barra, A. L.; Brunel, L. C.; Guillot, M. Alternating current susceptibility, high field magnetization, and millimeter band EPR evidence for a ground S = 10 state in [Mn$_{12}$O$_{12}$(CH$_3$COO)$_{16}$(H$_2$O)$_4$]·2CH$_3$COOH·4H$_2$O. *J. Am. Chem. Soc.* **1991**, *113*, 5873. (b) Sessoli, R.; Tsai, H. L.; Schake, A. R.; Wang, S.; Vincent, J. B.; Folting, K.; Gatteschi, D.; Christou, G.; Hendrickson, D. N. High-spin molecules: [Mn$_{12}$O$_{12}$(O$_2$CR)$_{16}$(H$_2$O)$_4$]. *J. Am. Chem. Soc.* **1993**, *115*, 1804−1816. (c) Sessoli, R.; Gatteschi, D.; Caneschi, A.; Novak, M. A. Magnetic bistability in a metal-ion cluster. *Nature* **1993**, *365*, 141−143.

(3) (a) Leuenberger, M. N.; Loss, D. Quantum computing in molecular magnets. *Nature* **2001**, *410*, 789−793. (b) Troiani, F.; Affronte, M. Molecular spins for quantum information technologies. *Chem. Soc. Rev.* **2011**, *40*, 3119. (c) Hao, H.; Zheng, X.; Jia, T.; Zeng, Z. Room temperature memory device using single-molecule magnets. *RSC Adv.* **2015**, *5*, 54667−54671. (d) Atzori, M.; Sessoli, R. The Second Quantum Revolution: Role and Challenges of Molecular Chemistry. *J. Am. Chem. Soc.* **2019**, *141*, 11339−11352. (e) Moreno-Pineda, E.; Wernsdorfer, W. Measuring molecular magnets for quantum technologies. *Nat. Rev. Phys.* **2021**, *3*, 645−659.

(4) (a) Bogani, L.; Wernsdorfer, W. *Molecular spintronics using single-molecule magnets*. *Nanoscience and Technology*; Co-Published with Macmillan Publishers Ltd, UK, 2009; pp 194−201. (b) Hu, J.; Wu, R. Giant Magnetic Anisotropy of Transition-Metal Dimers on Defected Graphene. *Nano Lett.* **2014**, *14*, 1853−1858. (c) Hirohata, A.; Yamada,

K.; Nakatani, Y.; Prejbeanu, I.-L.; Diény, B.; Pirro, P.; Hillebrands, B. Review on spintronics: Principles and device applications. *J. Magn. Magn. Mater.* **2020**, *509*, 166711.

(5) (a) Lunghi, A.; Totti, F.; Sessoli, R.; Sanvito, S. The role of anharmonic phonons in under-barrier spin relaxation of single molecule magnets. *Nat. Commun.* **2017**, *8*, 14620. (b) Castro-Alvarez, A.; Gil, Y.; Llanos, L.; Aravena, D. High performance single-molecule magnets, Orbach or Raman relaxation suppression? *Inorg. Chem. Front.* **2020**, *7*, 2478−2486.

(6) (a) Gomez-Coca, S.; Cremades, E.; Aliaga-Alcalde, N.; Ruiz, E. Mononuclear Single-Molecule Magnets: Tailoring the Magnetic Anisotropy of First-Row Transition-Metal Complexes. *J. Am. Chem. Soc.* **2013**, *135*, 7010−7018. (b) Craig, G. A.; Murrie, M. 3d single-ion magnets. *Chem. Soc. Rev.* **2015**, *44*, 2135−2147. (c) Frost, J. M.; Harriman, K. L. M.; Murugesu, M. The rise of 3-d single-ion magnets in molecular magnetism: towards materials from molecules? *Chem. Sci.* **2016**, *7*, 2470−2491. (d) Freedman, D. E.; Harman, W. H.; Harris, T. D.; Long, G. J.; Chang, C. J.; Long, J. R. Slow Magnetic Relaxation in a High-Spin Iron(II) Complex. *J. Am. Chem. Soc.* **2010**, *132*, 1224−1225. (e) Harman, W. H.; Harris, T. D.; Freedman, D. E.; Fong, H.; Chang, A.; Rinehart, J. D.; Ozarowski, A.; Sougrati, M. T.; Grandjean, F.; Long, G. J.; Long, J. R.; Chang, C. J. Slow Magnetic Relaxation in a Family of Trigonal Pyramidal Iron(II) Pyrrolide Complexes. *J. Am. Chem. Soc.* **2010**, *132*, 18115−18126. (f) Marriott, K. E. R.; Bhaskaran, L.; Wilson, C.; Medarde, M.; Ochsenbein, S. T.; Hill, S.; Murrie, M. Pushing the limits of magnetic anisotropy in trigonal bipyramidal Ni(II). *Chem. Sci.* **2015**, *6*, 6823−6828. (g) Landart-Gereka, A.; Quesada-Moreno, M. M.; Díaz-Ortega, I. F.; Nojiri, H.; Ozerov, M.; Krzystek, J.; Palacios, M. A.; Colacio, E. Large easy-axis magnetic anisotropy in a series of trigonal prismatic mononuclear cobalt(II) complexes with zero-field hidden single-molecule magnet behaviour: the important role of the distortion of the coordination sphere and intermolecular interactions in the slow relaxation. *Inorg. Chem. Front.* **2022**, *9*, 2810−2831.

(7) (a) Rinehart, J. D.; Long, J. R. Exploiting single-ion anisotropy in the design of f-element single-molecule magnets. *Chem. Sci.* **2011**, *2*, 2078. (b) Woodruff, D. N.; Winpenny, R. E. P.; Layfield, R. A. Lanthanide Single-Molecule Magnets. *Chem. Rev.* **2013**, *113*, 5110−5148. (c) Layfield, R. A., Murugesu, M., Eds. *Lanthanides and Actinides in Molecular Magnetism: Layfield/Lanthanides and Actinides in Molecular Magnetism*; Wiley-VCH Verlag GmbH & Co. KGaA: Weinheim, Germany, 2015. (d) Zhu, Z.; Guo, M.; Li, X.-L.; Tang, J. Molecular magnetism of lanthanide: Advances and perspectives. *Coord. Chem. Rev.* **2019**, *378*, 350−364. (e) Ding, X.-L.; Zhai, Y.-Q.; Han, T.; Chen, W.-P.; Ding, Y.-S.; Zheng, Y.-Z. A Local D_{4h} Symmetric Dysprosium(III) Single-Molecule Magnet with an Energy Barrier Exceeding 2000 K. *Chem.—Eur. J.* **2021**, *27*, 2623−2627. (f) Ishikawa, N.; Sugita, M.; Ishikawa, T.; Koshihara, S.-y.; Kaizu, Y. Lanthanide Double-Decker Complexes Functioning as Magnets at the Single-Molecular Level. *J. Am. Chem. Soc.* **2003**, *125*, 8694−8695. (g) Liu, J.; Chen, Y.-C.; Liu, J.-L.; Vieru, V.; Ungur, L.; Jia, J.-H.; Chibotaru, L. F.; Lan, Y.; Wernsdorfer, W.; Gao, S.; Chen, X.-M.; Tong, M.-L. A Stable Pentagonal Bipyramidal Dy(III) Single-Ion Magnet with a Record Magnetization Reversal Barrier over 1000 K. *J. Am. Chem. Soc.* **2016**, *138*, 5441−5450. (h) Canaj, A. B.; Dey, S.; Martí, E. R.; Wilson, C.; Rajaraman, G.; Murrie, M. Insight into D_{6h} Symmetry: Targeting Strong Axiality in Stable Dysprosium(III) Hexagonal Bipyramidal Single-Ion Magnets. *Angew. Chem., Int. Ed.* **2019**, *58*, 14146−14151. (i) Li, Z.; Zhai, Y.; Chen, W.; Ding, Y.; Zheng, Y. Air-Stable Hexagonal Bipyramidal Dysprosium(III) Single-Ion Magnets with Nearly Perfect D_{6h} Local Symmetry. *Chem.—Eur. J.* **2019**, *25*, 16219−16224. (j) Moreno-Pineda, E.; Nodaraki, L. E.; Tuna, F. Molecular Nanomagnets Based on f-Elements. *Novel Magnetic Nanostructures*; Elsevier, 2018; pp 1−50. (k) Zhu, Z.; Tang, J. Lanthanide single-molecule magnets with high anisotropy barrier: where to from here? *Natl. Sci. Rev.* **2022**, nwac194.

(8) Chiesa, A.; et al. Understanding magnetic relaxation in single-ion magnets with high blocking temperature. *Phys. Rev. B* **2020**, *101*, 174402.

(9) Zadrozny, J. M.; Xiao, D. J.; Atanasov, M.; Long, G. J.; Grandjean, F.; Neese, F.; Long, J. R. Magnetic blocking in a linear iron(I) complex. *Nature Chem.* **2013**, *5*, 577−581.

(10) Randall McClain, K.; Gould, C. A.; Chakarawet, K.; Teat, S. J.; Groshens, T. J.; Long, J. R.; Harvey, B. G. High-temperature magnetic blocking and magneto-structural correlations in a series of dysprosium-(III) metallocenium single-molecule magnets. *Chem. Sci.* **2018**, *9*, 8492−8503.

(11) (a) Yao, X.-N.; Du, J.-Z.; Zhang, Y.-Q.; Leng, X.-B.; Yang, M.-W.; Jiang, S.-D.; Wang, Z.-X.; Ouyang, Z.-W.; Deng, L.; Wang, B.-W.; Gao, S. Two-Coordinate Co(II) Imido Complexes as Outstanding Single-Molecule Magnets. *J. Am. Chem. Soc.* **2017**, *139*, 373−380. (b) Guo, F.-S.; Day, B. M.; Chen, Y.-C.; Tong, M.-L.; Mansikkamäki, A.; Layfield, R. A. Magnetic hysteresis up to 80 K in a dysprosium metallocene single-molecule magnet. *Science* **2018**, *362*, 1400−1403. (c) Zhu, Z.; Zhao, C.; Feng, T.; Liu, X.; Ying, X.; Li, X.-L.; Zhang, Y.-Q.; Tang, J. Air-Stable Chiral Single-Molecule Magnets with Record Anisotropy Barrier Exceeding 1800 K. *J. Am. Chem. Soc.* **2021**, *143*, 10077−10082. (d) Liu, S.; Gil, Y.; Zhao, C.; Wu, J.; Zhu, Z.; Li, X.-L.; Aravena, D.; Tang, J. A conjugated Schiff-base macrocycle weakens the transverse crystal field of air-stable dysprosium single-molecule magnets. *Inorg. Chem. Front.* **2022**, *9*, 4982−4989. (e) Zhu, Z.; Ying, X.; Zhao, C.; Zhang, Y.-Q.; Tang, J. A new breakthrough in low-coordinate Dy(III) single-molecule magnets. *Inorg. Chem. Front.* **2022**, DOI: 10.1039/D2QI01940J.

(12) (a) Dreiser, J. Molecular lanthanide single-ion magnets: from bulk to submonolayers. *J. Phys.: Condens. Matter* **2015**, *27*, 183203. (b) Wäckerlin, C.; Donati, F.; Singha, A.; Baltic, R.; Rusponi, S.; Diller, K.; Patthey, F.; Pivetta, M.; Lan, Y.; Klyatskaya, S.; Ruben, M.; Brune, H.; Dreiser, J. Giant Hysteresis of Single-Molecule Magnets Adsorbed on a Nonmagnetic Insulator. *Adv. Mater.* **2016**, *28*, 5195−5199. (c) Studniarek, M.; Wäckerlin, C.; Singha, A.; Baltic, R.; Diller, K.; Donati, F.; Rusponi, S.; Brune, H.; Lan, Y.; Klyatskaya, S.; Ruben, M.; Seitsonen, A. P.; Dreiser, J. Understanding the Superior Stability of Single-Molecule Magnets on an Oxide Film. *Adv. Sci.* **2019**, *6*, 1901736. (d) Diller, K.; Singha, A.; Pivetta, M.; Wäckerlin, C.; Hellwig, R.; Verdini, A.; Cossaro, A.; Floreano, L.; Vélez-Fort, E.; Dreiser, J.; Rusponi, S.; Brune, H. Magnetic properties of on-surface synthesized single-ion molecular magnets. *RSC Adv.* **2019**, *9*, 34421−34429.

(13) (a) Ou, X.; Wang, H.; Fan, F.; Li, Z.; Wu, H. Giant Magnetic Anisotropy of Co, Ru, and Os Adatoms on MgO (001) Surface. *Phys. Rev. Lett.* **2015**, *115*, 257201. (b) Donati, F.; et al. Magnetic remanence in single atoms. *Science* **2016**, *352*, 318−321. (c) Karbowiak, M.; Rudowicz, C. Ground state of Ho atoms on Pt(111) metal surfaces: Implications for magnetism. *Phys. Rev. B* **2016**, *93*, 184415. (d) Zhang, K.-C.; Li, Y.-F.; Liu, Y.; Zhu, Y.; Shi, L.-B. Giant magnetic anisotropy of rare-earth adatoms and dimers adsorbed by graphene oxide. *Phys. Chem. Chem. Phys.* **2017**, *19*, 13245−13251. (e) Rudowicz, C.; Tadyszak, K.; Slusarski, T.; Verissimo-Alves, M.; Kozanecki, M. Modeling Spin Hamiltonian Parameters for Fe^{2+} (S = 2) Adatoms on Cu$_2$N/Cu(100) Surface Using Semiempirical and Density Functional Theory Approaches. *Appl. Magn. Reson.* **2019**, *50*, 769−783. (f) Zuo, P.; Wang, H.; Wang, Z.; Wu, R. Large magnetic anisotropy of single transition metal adatoms on WS$_2$. *J. Magn. Magn. Mater.* **2020**, *506*, 166796.

(14) Georgiev, M.; Chamati, H. Fine structure and the huge zero-field splitting in Ni^{2+} complexes. Under preparation.

(15) Ashebr, T. G.; Li, H.; Ying, X.; Li, X.-L.; Zhao, C.; Liu, S.; Tang, J. Emerging Trends on Designing High-Performance Dysprosium(III) Single-Molecule Magnets. *ACS Materials Lett.* **2022**, *4*, 307−319.

(16) (a) Feng, M.; Tong, M.-L. Single Ion Magnets from 3d to 5f: Developments and Strategies. *Chem.—Eur. J.* **2018**, *24*, 7574−7594. (b) Hołyńska, M. *Single-molecule magnets: molecular architectures and building blocks for spintronics*; Wiley: Weinheim, 2019. (c) Shao, D.; Wang, X. Development of Single-Molecule Magnets. *Chin. J. Chem.* **2020**, *38*, 1005−1018. (d) Perlepe, P. S.; Maniaki, D.; Pilichos, E.; Katsoulakou, E.; Perlepes, S. P. Smart Ligands for Efficient 3d-, 4d- and 5d-Metal Single-Molecule Magnets and Single-Ion Magnets. *Inorganics* **2020**, *8*, 39. (e) Kalita, P.; Acharya, J.; Chandrasekhar, V. Mononuclear

pentagonal bipyramidal Ln(III) complexes: Syntheses and magnetic properties. *J. Magn. Magn. Mater.* **2020**, *498*, 166098. (f) Zhuo, Z.; Li, G.; Huang, Y.Understanding Magneto-Structural Correlations Toward Design of Molecular Magnets. In *Advanced Structural Chemistry*; Cao, R., Ed.; Wiley, 2021; pp 777−832.

(17) Luo, Q.-C.; Zheng, Y.-Z. Methods and Models of Theoretical Calculation for Single-Molecule Magnets. *Magnetochemistry* **2021**, *7*, 107.

(18) (a) Ghassemi Tabrizi, S.; Arbuznikov, A. V.; Kaupp, M. Exact Mapping from Many-Spin Hamiltonians to Giant-Spin Hamiltonians. *Chem.—Eur. J.* **2018**, *24*, 4689−4702. (b) Postnikov, A. V.; Kortus, J.; Pederson, M. R. Density functional studies of molecular magnets. *Phys. Status Solidi B* **2006**, *243*, 2533−2572. (c) Maurice, R.; de Graaf, C.; Guihéry, N. Magnetic anisotropy in binuclear complexes in the weak-exchange limit: From the multispin to the giant-spin Hamiltonian. *Phys. Rev. B* **2010**, *81*, 214427.

(19) Georgiev, M.; Chamati, H. Origin of the magnetic exchange in insulators: Localized vs. delocalized electrons. *J. Phys.: Conf. Ser.* **2021**, *1762*, 012019.

(20) (a) Abragam, A.; Bleaney, B.*Electron paramagnetic resonance of transition ions*; Oxford classic texts in the physical sciences; Oxford University Press: Oxford, 2012. (b) de Graaf, C.; Broer, R.*Magnetic Interactions in Molecules and Solids*; Theoretical Chemistry and Computational Modelling; Springer International Publishing: Cham, 2016.

(21) (a) Kahn, O.*Molecular magnetism*, 4th ed.; Wiley-VCH: New York, 2001. (b) Boča, R.*Theoretical Foundations of Molecular Magnetism*; Elsevier: Burlington, 1999.

(22) (a) Rudowicz, C. Concept of spin Hamiltonian, forms of zero-field splitting and electron Zeeman Hamiltonians and relations between parameters used in EPR. A critical review. *Mag. Res. Rev.* **1987**, *13*, 1−89. (b) Rudowicz, C. Erratum. *Mag. Res. Rev.* **1988**, *13*, 335.

(23) (a) Xu, Y.; Yang, G.-L.; Chu, D.-P.; Zhai, H.-R. Theory of the Single Ion Magnetocrystalline Anisotropy of 3d Ions. *Phys. Status Solidi B* **1990**, *157*, 685−693. (b) Rudowicz, C.; Tadyszak, K.; Ślusarski, T. Can the correspondence principle lead to improper relations between the uniaxial magnetic anisotropy constant K and the axial zero-field splitting parameter D for adatoms on surfaces? *J. Magn. Magn. Mater.* **2019**, *471*, 89−96. (c) Boča, R.; Rajnák, C. Unexpected behavior of single ion magnets. *Coord. Chem. Rev.* **2021**, *430*, 213657.

(24) (a) Kittel, C.*Quantum Theory of Solids*, 2nd ed.; Wiley: New York, 1987. (b) Jensen, J.; Mackintosh, A. R.*Rare Earth Magnetism: Structures and Excitations*; International Series of Monographs on Physics; Clarendon: Oxford, New York, 1991; Vol. *81*.

(25) Buschow, K. H. J.; de Boer, F. R.*Physics of magnetism and magnetic materials*; Kluwer: New York, 2003.

(26) Kittel, C.*Introduction to Solid State Physics*, 8th ed.; Wiley: New York, 2005.

(27) (a) White, R.*Quantum theory of magnetism: magnetic properties of materials*; Springer Series in Solid-State Sciences; Springer: Berlin, 2007; Vol. *32*. (b) Rudowicz, C.; Karbowiak, M. Disentangling intricate web of interrelated notions at the interface between the *physical* (crystal field) Hamiltonians and the *effective* (spin) Hamiltonians. *Coord. Chem. Rev.* **2015**, *287*, 28−63.

(28) (a) Rudowicz, C.; Karbowiak, M. Terminological confusions and problems at the interface between the crystal field Hamiltonians and the zero-field splitting Hamiltonians—Survey of the CF = ZFS confusion in recent literature. *Phys. B: Condens. Matter* **2014**, *451*, 134−150. (b) Rudowicz, C.; Karbowiak, M. Revealing the consequences and errors of substance arising from the inverse confusion between the crystal (ligand) field quantities and the zero-field splitting ones. *Phys. B: Condens. Matter* **2015**, *456*, 330−338.

(29) (a) Boča, R.*Magnetic Parameters and Magnetic Functions in Mononuclear Complexes Beyond the Spin-Hamiltonian Formalism*. In *Magnetic Functions Beyond the Spin-Hamiltonian*; Mingos, D. M. P., Ed.; Springer-Verlag: Berlin/Heidelberg, 2006; Vol. *117*; pp 1−264. (b) Kubica, A.; Kowalewski, J.; Kruk, D.; Odelius, M. Zero-field splitting in nickel(II) complexes: A comparison of DFT and multi-

configurational wavefunction calculations. *J. Chem. Phys.* **2013**, *138*, 064304.

(30) (a) Ma, D.; Li Manni, G.; Gagliardi, L. The generalized active space concept in multiconfigurational self-consistent field methods. *J. Chem. Phys.* **2011**, *135*, 044128. (b) Georgiev, M.; Chamati, H. Molecular magnetism in the multi-configurational self-consistent field method. *J. Phys.: Condens. Matter* **2021**, *33*, 075803. (c) Georgiev, M.; Chamati, H. Magnetostructural Dependencies in $3d^2$ Systems: The Trigonal Bipyramidal V^{3+} Complex. *Phys. Status Solidi B* **2022**, *259*, 2100645.

(31) (a) Labanowski, J. K., Andzelm, J. W., Eds. *Density Functional Methods in Chemistry*; Springer New York: New York, NY, 1991. (b) Ciofini, I. DFT calculations of molecular magnetic properties of coordination compounds. *Coord. Chem. Rev.* **2003**, *238−239*, 187−209. (c) Orio, M.; Pantazis, D. A.; Neese, F. Density functional theory. *Photosynth Res.* **2009**, *102*, 443−453. (d) Ferré, N., Filatov, M., Huix-Rotllant, M., Eds. *Density-Functional Methods for Excited States*, 1st ed.; Topics in Current Chemistry; Springer International Publishing: Imprint: Springer: Cham, 2016.

(32) (a) Prather, J. L.*Atomic Energy Levels in Crystals*; United States Government Printing Office, 1961. (b) Yosida, K.*Theory of magnetism*; Springer series in solid-state sciences; Springer: Berlin, New York, 1996. (c) Coey, J. M. D.*Magnetism and magnetic materials*; Cambridge University Press: New York, 2010. (d) Miessler, G. L.; Fischer, P. J.; Tarr, D. A.*Inorganic chemistry*, 5th ed.; Pearson: Boston, 2014. (e) Clemente-Juan, J. M.; Coronado, E.; Gaita-Ariño, A.*Mononuclear Lanthanide Complexes: Use of the Crystal Field Theory to Design Single-Ion Magnets and Spin Qubits*. In *Lanthanides and Actinides in Molecular Magnetism*; Layfield, R. A., Murugesu, M., Eds.; Wiley-VCH Verlag GmbH & Co. KGaA: Weinheim, Germany, 2015; pp 27−60.

(33) Weber, H. J.; Arfken, G. B.*Essential Mathematical Methods for Physicists*; Elsevier Science: Saint Louis, MO, 2014.

(34) (a) Ruamps, R.; Maurice, R.; Batchelor, L.; Boggio-Pasqua, M.; Guillot, R.; Barra, A. L.; Liu, J.; Bendeif, E.-E.; Pillet, S.; Hill, S.; Mallah, T.; Guihéry, N. Giant Ising-Type Magnetic Anisotropy in Trigonal Bipyramidal Ni(II) Complexes: Experiment and Theory. *J. Am. Chem. Soc.* **2013**, *135*, 3017−3026. (b) Gómez-Coca, S.; Cremades, E.; Aliaga-Alcalde, N.; Ruiz, E. Huge Magnetic Anisotropy in a Trigonal-Pyramidal Nickel(II) Complex. *Inorg. Chem.* **2014**, *53*, 676−678. (c) Craig, G. A.; Sarkar, A.; Woodall, C. H.; Hay, M. A.; Marriott, K. E. R.; Kamenev, K. V.; Moggach, S. A.; Brechin, E. K.; Parsons, S.; Rajaraman, G.; Murrie, M. Probing the origin of the giant magnetic anisotropy in trigonal bipyramidal Ni(II) under high pressure. *Chem. Sci.* **2018**, *9*, 1551−1559.

(35) (a) Georgiev, M.; Chamati, H. Magnetic excitations in molecular magnets with complex bridges: The tetrahedral molecule Ni_4Mo_{12}. *Eur. Phys. J. B* **2019**, *92*, 93. (b) Georgiev, M.; Chamati, H. Magnetization steps in the molecular magnet Ni_4Mo_{12} revealed by complex exchange bridges. *Phys. Rev. B* **2020**, *101*, 094427. (c) Georgiev, M.; Chamati, H. An Exchange Mechanism for the Magnetic Behavior of Er^{3+} Complexes. *Molecules* **2021**, *26*, 4922.